Linear–scaling implementation of exact exchange using localized numerical orbitals and contraction reduction integrals

Lionel A. Truflandier*
London Centre for Nanotechnology, UCL, 17-19 Gordon Street, London WC1H 0AH, UK and
Thomas Young Centre and Department of Physics & Astronomy, UCL, Gower Street, London WC1E 6BT, UK†

Tsuyoshi Miyazaki
National Institute for Materials Science, 1-2-1 Sengen, Tsukuba, Ibaraki 305-0045, Japan

David R. Bowler‡
London Centre for Nanotechnology, UCL, 17-19 Gordon Street, London WC1H 0AH, UK
Thomas Young Centre and Department of Physics & Astronomy,
UCL, Gower Street, London WC1E 6BT, UK† *and*
International Center for Materials Nanoarchitectonics,
National Institute for Materials Science, 1-1 Namiki, Tsukuba, Ibaraki 305-0044, Japan
(Dated: November 13, 2012)

We present enhancements to the computational efficiency of exact exchange calculations using the density matrix and local support functions. We introduce a numerical method which avoids the explicit calculation the four-center two-electron repulsion integrals and reduces the prefactor scaling by a factor N, where N is the number of atoms within the range of the exact exchange Hamiltonian. This approach is based on a contraction-reduction scheme, and takes advantage of the discretization space which enables the direct summation over the support functions in a localized space. Using the sparsity property of the density matrix, the scaling of the prefactor can be further reduced to reach asymptotically $O(N)$.

PACS numbers: 71.15.Dx 71.15.Ap 71.15.Mb 02.60.Jh

The calculation of exchange energy as found in the "Fock–exchange" for Hartree–Fock (HF) theory or "exact–exchange" for Kohn–Sham (KS) density functional theory (DFT) is well-known to be time consuming, where for a naive implementation the scaling increases with the fourth power of the number of atoms, N, or the number of basis states. It has therefore been the focus of considerable efforts to improve both the efficiency and the scaling. Much of the work has taken place within the quantum chemistry community focussing on approaches using Gaussian-type orbitals (GTO) or exponential-type functions for the radial part such as the well-known Slater-type orbitals (STO). More recently, there has been interest in efficient implementation within the periodic density functional theory community, which traditionally use plane waves as basis functions (along with atomic pseudopotentials) and required discrete fast Fourier transform (FFT) technologies. At the same time, linear scaling, or $O(N)$, approaches to finding the electronic ground state have emerged over the last ten to fifteen years,[1,2] and new schemes for the evaluation of exact exchange energy have to be developed including the specifications of the $O(N)$ techniques. We report a novel approach to improving the efficiency of exchange calculations for *any* localised basis functions, which fits naturally within the formalism of linear scaling DFT calculations ; more specifically with the code CONQUEST[3–5].

Within the framework of the HF theory, the exchange energy for a closed-shell system can be written as:

$$E_x = -\frac{1}{4}\int d\mathbf{r}d\mathbf{r}'\frac{\rho(\mathbf{r},\mathbf{r}')\rho(\mathbf{r}',\mathbf{r})}{|\mathbf{r}-\mathbf{r}'|}, \tag{1}$$

using the definition of the density matrix in terms of the molecular eigenstates $\psi_n(\mathbf{r})$,

$$\rho(\mathbf{r},\mathbf{r}') = 2\sum_n \psi_n(\mathbf{r}')\psi_n^\star(\mathbf{r}), \tag{2}$$

where n runs over the doubly occupied orbitals. This yields a more explicit expression for the exchange energy:

$$E_x = -\sum_{nm}\int d\mathbf{r}d\mathbf{r}'\frac{\psi_m^\star(\mathbf{r})\psi_n^\star(\mathbf{r}')\psi_n(\mathbf{r})\psi_m(\mathbf{r}')}{|\mathbf{r}-\mathbf{r}'|}. \tag{3}$$

The typical procedure in quantum chemistry is to express the exchange energy of Eq. (3) in terms of 4-center 2-electron repulsion integrals (ERI) by expanding $\psi_n(\mathbf{r})$ onto a linear combination of real atom-centered functions $\varphi_i(\mathbf{r})$. Using the standard notation, the ERI formally reads:

$$(ik|lj) = \int d\mathbf{r}d\mathbf{r}'\frac{\varphi_i(\mathbf{r})\varphi_k(\mathbf{r})\varphi_l(\mathbf{r}')\varphi_j(\mathbf{r}')}{|\mathbf{r}-\mathbf{r}'|} \tag{4}$$

The earliest approaches to linear scaling exchange used pre-screening on the integrals and the density matrix based on an assumed decay rate ; see for instance the LinK[6] and ONX[7,8] algorithms. These analytical methods have been successfully applied in various quantum chemistry codes, though relying on specific basis sets such as

Gaussian-type orbitals (GTO). Alternative efficient solutions generally make the use of a 3-center reduction scheme,[9–13] deriving from the density-fitting approach of Baerends and Roos for Slater-type orbtials (STO),[14] and Dunlap and coworkers[15,16] for GTO basis sets. Different approaches with a similar spirit, such as the pseudo–spectral[17,18] or the resolution of identity methods[19,20] have also demonstrated to be efficient, and improvements are still explored by many groups.[13,21,22]

The plane wave basis sets common within periodic DFT implementations make these approaches impossible, and most implementations concentrate on reciprocal space using FFTs.[23–25] It should be mentioned here that acceptable accuracy is obtained only if an adequate treatment of the Coulomb singularities are considered.[26–30]. Recently, using a transformation of the Kohn-Sham orbitals to maximally localised Wannier functions, a linear scaling calculation of the exchange potential has been demonstrated.[31] Localised numerical orbital DFT approaches to exchange include the semi-analytic solution given by Toyoda and Ozaki[32,33] combining fast-spherical Bessel transform for the radial integration and a more traditional analytic method for the spherical harmonic part. A numerical scheme has also been proposed by Shang et al.[34] where ERI are computed by solving numerically the Poisson's equation for each localized pair-density $\rho_{lj} = \varphi_l \varphi_j$, and integrating in real space. Similarly to planewave periodic exchange calculations, the main drawback resides in the accuracy of the Poisson solver. All the methods outlined above involves the explicit calculation of the full or screened set of ERIs.

We introduce instead a route which circumvents the calculation of the four-center integrals and works for any smooth finite-range functions, which is particulary well suited for $O(N)$ approaches. In standard linear scaling theory, the density matrix is used as the fundamental variable and is written in a separable form in terms of localised orbitals, also called support functions $\phi_i(\mathbf{r})$,

$$\rho(\mathbf{r}, \mathbf{r}') = 2 \sum_{ij} \phi_i(\mathbf{r}) K_{ij} \phi_j(\mathbf{r}') \tag{5}$$

where K_{ij} is the density matrix in the representation of the support functions, also known as the density kernel. Linear scaling is achieved when the support functions, centred on the atomic positions R_i, are strictly localised in space and a cutoff is applied to K_{ij} so that,

$$K_{ij} = 0 \text{ for } |R_i - R_j| > R_K, \tag{6}$$

with R_K the density matrix range. From Eq. (5) we can therefore write the exchange energy as:

$$E_x = -\sum_{ijkl} \int d\mathbf{r} d\mathbf{r}' \frac{\phi_i(\mathbf{r}) K_{ij} \phi_j(\mathbf{r}') \phi_k(\mathbf{r}) K_{kl} \phi_l(\mathbf{r}')}{|\mathbf{r} - \mathbf{r}'|} \tag{7}$$

$$= -\sum_{ij} K_{ij} X_{ij} \tag{8}$$

with,

$$X_{ij} = \sum_{kl} \int d\mathbf{r} d\mathbf{r}' \frac{\rho_{ik}(\mathbf{r}) K_{kl} \rho_{lj}(\mathbf{r}')}{|\mathbf{r} - \mathbf{r}'|}. \tag{9}$$

The exchange matrix X becomes now the key quantity to calculate, and for $R_K \to \infty$, the resulting exchange energy must be exact. We note that this form involves a contraction between K and one set of local orbitals, seen as the sum over l (or k) in Eq. (9). This type of contraction is frequently performed in CONQUEST[35], but in this case will reduce the prefactor for exchange energy calculation by removing one of the four centres of the ERI. Moreover, if we apply a range R_X to the exchange, such as

$$X_{ij} = 0 \text{ for } |R_i - R_j| > R_X, \tag{10}$$

we can then achieve linear scaling with the prefactor depending on the localisation of the matrix. The resulting method is not only efficient, but should be scalable in parallel, as it is compatible with the standard CONQUEST approach to matrix and support function operations.

As mentioned in the introduction, the key part is to perform the sum over the index l *before* solving for the Coulomb potential of the pair densities; this simple re-ordering increases the efficiency of the procedure markedly, as we will show below. We define new contraction functions, $\Phi_k(\mathbf{r}')$, as:

$$\Phi_k(\mathbf{r}') = \sum_l K_{kl} \phi_l(\mathbf{r}') \tag{11}$$

It should be outlined that the domain over which these functions are defined requires some care; this is detailed in the Appendix. The sum over l need only include those support functions ϕ_l overlapping with ϕ_j, as Φ_k will be multiplied by this function. Contracted densities are then defined as:

$$\bar{\rho}_{kj}(\mathbf{r}') = \Phi_k(\mathbf{r}') \phi_j(\mathbf{r}'), \tag{12}$$

and the resulting Coulomb potential,

$$\bar{v}_{kj}(\mathbf{r}) = \int d\mathbf{r}' \frac{\bar{\rho}_{kj}(\mathbf{r}')}{|\mathbf{r} - \mathbf{r}'|}, \tag{13}$$

is calculated by solving Poisson's equation using, for instance, numerical FFT routines. As we discuss later, once the potential has been found a further contraction over k is performed to create the function $\Omega_j(\mathbf{r})$, as:

$$\Omega_j(\mathbf{r}) = \sum_k \bar{v}_{kj}(\mathbf{r}) \phi_k(\mathbf{r}), \tag{14}$$

where, again, the sum over support functions k need only include those functions which overlap with support function i. The matrix elements X_{ij} are then calculated by integration:

$$X_{ij} = \int d\mathbf{r} \phi_i(\mathbf{r}) \Omega_j(\mathbf{r}). \tag{15}$$

The set of function Ω_j is effectively defined by the density matrix range –normally applied to K_{kl} in accordance with Eq. (6)– and the need for j to overlap with atoms l. There is therefore a clear route to efficient linear scaling exchange calculations within the standard approaches of $O(N)$ electronic structure codes.

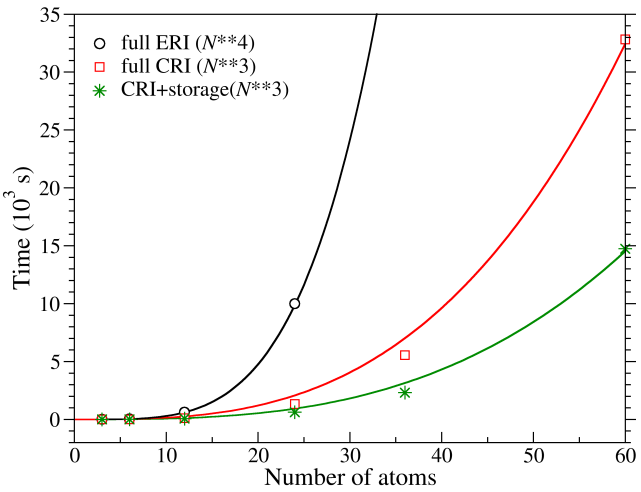

FIG. 1. Comparison of CPU times necessary to compute EXX in isolated water clusters as a function of number atoms (N) using explicit ERI calculation and the CRI method. Ideal N^4 and N^3 scalings are given by plain lines.

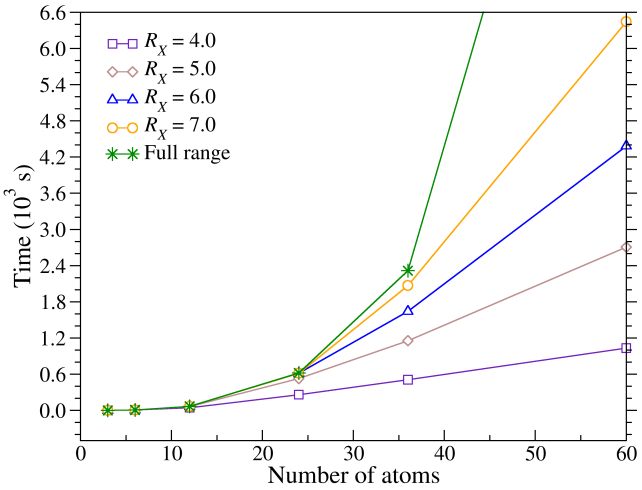

FIG. 2. Variation of CPU time with respect to the range R_X (in a.u.) for the calculation of EXX in isolated water clusters using the CRI method.

As previously remarked (see Eq. (10)), the calculation time can be reduced further with a screening condition on exchange matrix elements X_{ij}. This is related to the sparsity property of $\rho(\mathbf{r}, \mathbf{r}')$,[56] and the truncation of all the operators involved in the Hamiltonian.[57] From the algorithm of Fig. 5 (see Appendix), we note that the evaluation of the reduced potential $\bar{v}_{kj}$ is performed within a 3-index loop, which contrasts with the 4-index loop (over a limited set of atoms) used for the accumulation of temporary matrix Φ_k. Another possibility would be to compute and store the set $\{\phi_l\}$ (and $\{\phi_k\}$) once, reducing formally –after the first cycle– the execution time for the calculation of Φ_k to $N^3(N^2)$ but increasing the data storage by $N(N^2)$, respectively.

Practical tests on the efficiency of the contraction-reduction integral (CRI) algorithm were performed on a set of isolated water clusters $(H_2O)_n$ ($n \leq 20$) with fused cubes structures taken from the work of Wales and Hodges.[36] Calculations of exchange energy were realized after the KS density matrix has been converged using the standard self-consistent-field (SCF) method. As a result, the timings presented below for exact exchange (EXX) energy can be compared to a single SCF cycle as found in HF or hybrid-DFT calculation. For this demonstration, single-ζ numerical pseudo-atomic orbitals[37–39] (NAO) have been used for hydrogen and oxygen with cutoff radii of 4.7 and 3.8 au, respectively. We emphasize that the main conclusions of this work can be easily extended to more flexible basis sets, as far as the support functions are localized. SCF-KS and *post*-EXX calculations were performed with a fixed grid spacing of 0.25 au for the NAO discretization. This protocol allows us to realize fast enough computations on a single processor and also to draw qualitative conclusions on the exchange matrix range.

The central processing unit (CPU) times used for the computation of EXX are reported in Fig. 1 as a function of the number of atoms, for various water clusters, using: (i) the explicit evaluation of the full set of ERI, (ii) the CRI approach, and (iii) the CRI approach with partial storage of the NAO during the construction of the temporary matrix Φ_k involved in the 4-index loop (see Appendix). Comparing the formal scalings obtained for the CRI methods against the full ERI approach, it becomes clear that the contraction-reduction algorithm reduces the quartic scaling to to cubic scaling with respect to the size of the water clusters. Timings can be further reduced by requiring the storage of the NAOs (the set $\{\phi_l\}$). At this point we should emphasise that exchange energy values obtained with the three schemes are fully identical, their accuracies being only dependent on the Poisson solver used to evaluate the pair potential in Eq. (13).

Among the various numerical FFT-based methods, one can choose to evaluate the Coulomb potential in reciprocal or real space. Whereas the former is the most appropriate for periodic neutral systems –when the positively charged nuclei compensate exactly the electronic charge density– it becomes less efficient for isolated and/or charged systems.[40] Several schemes have been developed to tackle this problem,[41–44] Alternatives based on the discrete variable representation (DVR) of Eq. (13) which avoids the direct resolution of the Poisson equation have been proposed.[45] The density is generally expanded in a direct product of one-dimensional localized real-space

basis functions[45–47] as for instance, interpolating scaling functions (ISF). After extended comparisons between the DVR-ISF developed by Genovese et al.[48,49] and corrected reciprocal FFT-based schemes,[50–52] we found that systematic convergence of the ERI is obtained with a better accuracy and at a lower cost using the real space Poisson solver.[53]

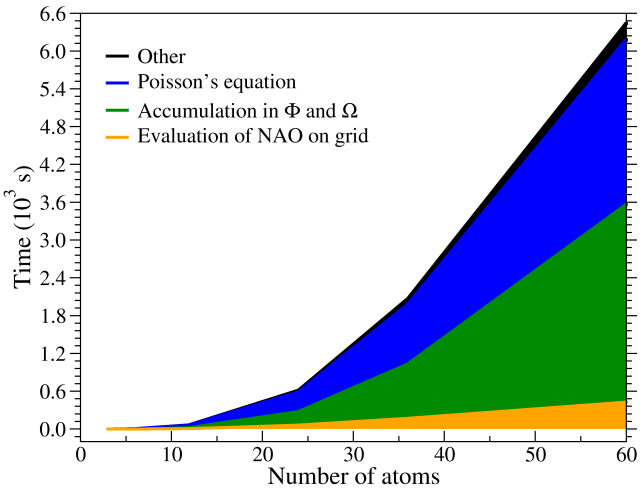

FIG. 3. Cumulative decomposition of the total execution time for EXX calculation in isolated water clusters using the CRI method along with the storage of the NAO and a screening of $R_X = 7.0$ au. Contributions of the three main routines are presented: the resolution of the Poisson equation, the accumulation in the temporary matrices Φ and Ω, and the NAO discretization .

As shown in Fig. 2, if integral screenings is introduced within the CRI algorithm –see Fig. 5 of the Appendix– the CPU time can be significantly reduced, allowing to reach the $O(N)$ regime for clusters with more than 36 atoms (at $R_X = 7.0$ au). Computational ressources further decrease for shorter EXX range along with the faster observation of the linear-scaling regime. Figure 3 presents the decomposition of the total execution time involved the calculation of the EXX using the CRI approach for $R_X = 7.0$ au. As it would be expected, most of the time is spent on the accumulation in the temporary matrices Φ_k and Ω_j, and the Poisson solver. Evaluation of the support functions on the cubic grid do not impact to much on timings as far as the reduced overlap space technique is considered (see Appendix).

The *post*-EXX accuracy with respect to R_X is given in Fig. 4 for the cluster $(H_2O)_{20}$ using the "boxkite" structure,[36] which is characterized by an edge length around 25.5 au. Because in the present study calculated EXX energy is not variational with respect to R_X, we do not expect a monotonic behavior for the plotted convergence profiles on Fig. 4, where an accuracy below 1 mHa is found for $R_X \geq 6.5$. This can be compared to the density matrix convergence of 10^{-7} Ha obtained at $R_K = 5.0$ au. As a result, the price to paid for the fast computation of exchange energy using the CRI algorithm is the reduction of the accuracy, which in our case is acceptable considering the size of the system. It should be mentioned that the constant exchange cutoff used in the 3-index loop of Fig. 5 can be different at the three stages. This will allow acceleration of the convergence without significantly affecting the efficiency. This linear scaling approach will scale in the same way as the other procedures in CONQUEST, opening the way to efficient exact exchange calculations on 100,000+ atoms.

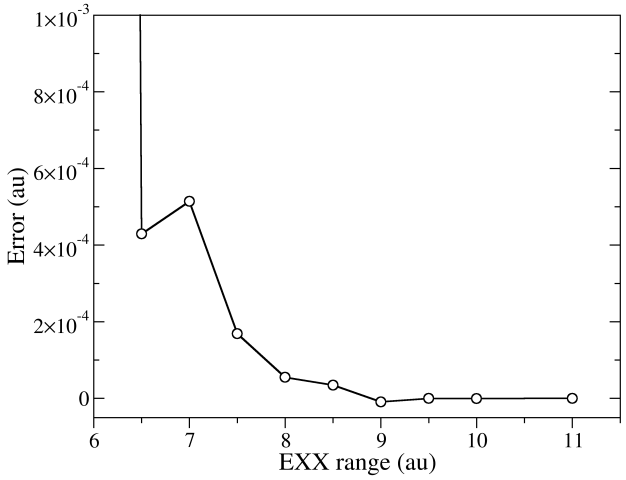

FIG. 4. Convergence of the *post*-EXX energy with respect to the exchange range R_X for the cluster $(H_2O)_{20}$. Error is given with respect to the exact calculation.

Finally, in this work we have shown that we are able to circumvent the N^4 scaling inferred by the standard calculation of exchange without any approximation. Even if the non-local nature of the EXX interaction requires a larger range compared to standard $O(N)$ DFT implementation, the linear-scaling regime is observable for a fair efficiency/accuracy ratio. In our case, computation time can be further reduced the fact that FFT-based Poisson' solvers are easily parallelizable along with a judicious choice of the EXX matrix range.

ACKNOWLEDGMENTS

L.A.T. was supported by the BBSRC grant BB/H024217/1, "Linear Scaling Density Functional Theory for Biochemistry". The authors are grateful to L. Tong, M. J. Gillan and M. Toyoda for useful discussions.

Appendix A: Implementation

To describe the practical implementation of the contraction-reduction integral algorithm we have to start from the explicit definition of the exchange matrix elements with respect to the ERIs and the basis set $\{\phi_i\}$. Within the discretized space Eq. (9) can be written as:

$$X_{ij} = \sum_{kl} K_{kl} \sum_{hg} \phi_i(\mathbf{r}_h - \mathbf{R}_i)\phi_k(\mathbf{r}_h - \mathbf{R}_k)\vartheta(\mathbf{r}_h, \mathbf{r}_g) \times \phi_l(\mathbf{r}_g - \mathbf{R}_l)\phi_j(\mathbf{r}_g - \mathbf{R}_j)w(\mathbf{r}_h)w(\mathbf{r}_g), \quad \text{(A1)}$$

where $\vartheta(\mathbf{r}_h, \mathbf{r}_g)$ represents the 2-electron Coulomb operator. We made explicit in Eq. (A1) the fact that the support functions are centered on the nuclei positions $\{\mathbf{R}_i\}$.

The sets $\{w(\mathbf{r}_h)\}$ and $\{w(\mathbf{r}_g)\}$ account for the weight factors of the quadrature points $\{\mathbf{r}_h\}$ and $\{\mathbf{r}_g\}$. We choose to work with an evenly spaced cubic grid where both $w(\mathbf{r}_h)$ and $w(\mathbf{r}_g)$ simplify to $w_{\text{int}} = h_{\text{int}}^3$, with h_{int} the grid spacing.[54] Under the translation $\mathbf{r} \to \mathbf{r} + \mathbf{R}_i$, which leaves invariant the ERI, we obtain

$$X_{ij} = \sum_{kl} K_{kl} \sum_{hg} \phi_i(\mathbf{r}_h)\phi_k(\mathbf{r}_h - \mathbf{R}_{ki})\vartheta(\mathbf{r}_h, \mathbf{r}_g) \times \phi_l(\mathbf{r}_g - \mathbf{R}_{li})\phi_j(\mathbf{r}_g - \mathbf{R}_{ji})w_{\text{int}}^2, \quad \text{(A2)}$$

using $\mathbf{R}_{ij} = \mathbf{R}_i - \mathbf{R}_j$. By virtue of the linearity of discretized space, we are allowed to introduce the temporary matrix:

$$\Phi_k(\mathbf{r}_g; \{\mathbf{R}_{li}\}) = \sum_l K_{kl}\phi_l(\mathbf{r}_g - \mathbf{R}_{li}). \quad \text{(A3)}$$

We emphasize that ϕ_l is evaluated on a cubic grid centered on the nucleus i. The explicit expression for the reduced density of Eq. (12) is given by,

$$\bar{\rho}_{kj}(\mathbf{r}_g; \mathbf{R}_{ji}, \{\mathbf{R}_{li}\}) = \Phi_k(\mathbf{r}_g)\phi_j(\mathbf{r}_g - \mathbf{R}_{ji}). \quad \text{(A4)}$$

The corresponding reduced pair potential $\bar{v}_{lj}$ is obtained by solving the Poisson equation. Finally, we introduce the temporary matrix:

$$\Omega_j(\mathbf{r}_h; \mathbf{R}_{ji}, \{\mathbf{R}_{li}\}, \{\mathbf{R}_{ki}\}) = \sum_k \phi_k(\mathbf{r}_h - \mathbf{R}_{ki})\bar{v}_{kj}(\mathbf{r}_h), \quad \text{(A5)}$$

to perform the last numerical integration, yielding the exchange matrix elements:

$$X_{ij}(\mathbf{r}_h; \mathbf{R}_{ji}, \{\mathbf{R}_{li}\}, \{\mathbf{R}_{ki}\}) = \sum_h \phi_i(\mathbf{r}_h)\Omega_j(\mathbf{r}_h)w_{\text{int}}. \quad \text{(A6)}$$

We have made the dependence of the various matrix elements on the translation vectors $\{\mathbf{R}_{ij}\}$ explicit. The CRI approach involves three main operations: (i) The projection of ϕ_i onto the discretized space, where both radial functions and spherical harmonics are evaluated on a cubic grid. (ii) The summations of Eqs. (A3) and (A5). (iii) The evaluation of the pair potential $\bar{v}_{kj}$.

FIG. 5. Algorithm describing exchange kernel formally scaling as N^3.

```
loop over atom i
    ▷ evaluate and ▷ store φ_i
    loop over atom j
        if R_ji < R_X then
            ▷ evaluate and ▷ store φ_j
            loop over atom k
                if R_ki < R_X then
                    ▷ evaluate φ_k and ▷ store ?
                    loop over atom l
                        ▷ fetch K_kl
                        if R_li < R_X then
                            ▷ evaluate φ_l and ▷ store ?
                            ◇ accumulate Φ_k
                        end if: R_X
                    end loop: l
                    ▷ calculate ρ̄_kj
                    ▷ evaluate v̄_kj
                    ◇ accumulate Ω_j
                end if: R_X
            end loop: k
        end if: R_X
    end loop: j
    ▷ integrate X_ij
end loop: i
```

The combination of local FFT grids[55] with the locality property of the NAO easily fulfils the efficiency requirement. On each *primary* atom i a box is centered at the position $\mathbf{R}_i$. This box contains an ensemble of grid points called $\mathcal{B}_i$. For the NAO set $\{j, k, l\}$ in Eq. (A2) other boxes $\mathcal{B}_a$ are defined and translated along the vector $\mathbf{R}_{ai}$. Here, we choose to work with identical cubic boxes of length $L \geq 2 \times r_c^{\max}$, where $r_c^{\max}$ is the largest confinement radius over the whole set of contracted support functions. Considering that the quadrature of Eq. (A2) is different from zero if significant overlap is deemed to exist between the orbital-pairs ik and lj, we can first reduced the computational resources involved in (i) by defining reduced spaces as,

$$\mathcal{O}_{ab} = \mathcal{B}_a \cap \mathcal{B}_b \quad \text{(A7)}$$

where $\mathcal{O}_{ab}$ is the overlap box of ϕ_a with ϕ_b. Then the discretization of $\{\phi_k, \phi_l\}$ is only realized for grid points common to the space span by ϕ_i and ϕ_k, respectively. Secondly, by using the fact that the coordinate system is centered on the primary atom, we can introduced an efficient screening during the course of the calculation and reduced the computational time related to (ii) and (iii). Accumulation in the temporary matrices Φ_k and Ω_j, which are centered on atom i, is performed if the distance R_{ai} between the two distribution centers is below the EXX cutoff R_X.

* l.truflandier@ism.u-bordeaux1.fr
† Present address: Institut des Sciences Moléculaires, Université Bordeaux I, 351 Cours de la Libération, 33405 Talence, France
‡ david.bowler@ucl.ac.uk

[1] C. Ochsenfeld, J. Kussmann, and D. S. Lambrecht, Reviews in Computational Chemistry **23**, 1 (2007).
[2] D. R. Bowler and T. Miyazaki, Reports on Progress in Physics **75**, 036503 (2012).
[3] D. R. Bowler, T. Miyazaki, and M. J. Gillan, J. Phys.: Condens. Matter **14**, 2781 (2002).
[4] T. Miyazaki, D. R. Bowler, R. Choudhury, and M. J. Gillan, J. Chem. Phys. **121**, 6186 (2004).
[5] D. R. Bowler, R. Choudhury, M. J. Gillan, and T. Miyazaki, phys. stat. sol. b **243**, 989 (2006), 10.1002/pssb.200541386.
[6] C. Ochsenfeld, C. A. White, and M. Head-Gordon, The Journal of Chemical Physics **109**, 1663 (1998).
[7] E. Schwegler and M. Challacombe, The Journal of Chemical Physics **105**, 2726 (1996).
[8] E. Schwegler, M. Challacombe, and M. Head-Gordon, The Journal of Chemical Physics **106**, 9708 (1997).
[9] R. Polly, H. Werner, F. R. Manby, and P. J. Knowles, Mol. Phys. **102**, 2311 (2004).
[10] F. Neese, F. Wennmohs, A. Hansen, and U. Becker, Chem. Phys. **356**, 98 (2009).
[11] M. A. Watson, N. C. Handy, and A. J. Cohen, J. Chem. Phys. **119**, 6475 (2003).
[12] M. Krykunov, T. Ziegler, and E. v. Lenthe, Int. J. Quantum Chem. **109**, 1676 (2009).
[13] R. A. Friesner, R. B. Murphy, M. D. Beachy, M. N. Ringnalda, W. T. Pollard, B. D. Dunietz, and Y. Cao, J. Phys. Chem. A **103**, 1913 (2011).
[14] E. Baerends, D. Ellis, and P. Ros, Chem. Phys. **2**, 41 (1973).
[15] B. I. Dunlap, J. W. D. Connolly, and J. R. Sabin, J. Chem. Phys. **71**, 3396 (1979).
[16] B. I. Dunlap, J. W. D. Connolly, and J. R. Sabin, J. Chem. Phys. **71**, 4993 (1979).
[17] F. Richard A., Chem. Phys. Lett. **116**, 39 (1985).
[18] R. A. Friesner, J. Chem. Phys. **85**, 1462 (1986).
[19] K. Eichkorn, O. Treutler, H. hm, M. Hser, and R. Ahlrichs, Chem. Phys. Lett. **242**, 652 (1995).
[20] K. Eichkorn, F. Weigend, O. Treutler, and R. Ahlrichs, Theor. Chem. Acc. **97**, 119 (1997).
[21] R. Izsak and F. Neese, J. Chem. Phys. **135**, 144105 (2011).
[22] S. Reine, E. Tellgren, A. Krapp, T. Kjrgaard, T. Helgaker, B. Jansik, S. Host, and P. Salek, J. Chem. Phys. **129**, 104101 (2008).
[23] F. Gygi and A. Baldereschi, Phys. Rev. B **34**, 4405 (1986).
[24] S. Chawla and G. A. Voth, J. Chem. Phys. **108**, 4697 (1998).
[25] J. Paier, R. Hirschl, M. Marsman, and G. Kresse, J. Chem. Phys. **122**, 234102 (2005).
[26] P. Broqvist, A. Alkauskas, and A. Pasquarello, Phys. Rev. B **80**, 085114 (2009).
[27] I. Duchemin and F. Gygi, Comp. Phys. Commun. **181**, 855 (2010).
[28] N. A. W. Holzwarth and X. Xu, Phys. Rev. B **84**, 113102 (2011).
[29] A. Sorouri, W. M. C. Foulkes, and N. D. M. Hine, J. Chem. Phys. **124**, 064105 (2006).
[30] J. Spencer and A. Alavi, Phys. Rev. B **77**, 193110 (2008).
[31] X. Wu, A. Selloni, and R. Car, Phys. Rev. B **79**, 085102 (2009).
[32] M. Toyoda and T. Ozaki, J. Chem. Phys. **130**, 124114 (2009).
[33] M. Toyoda and T. Ozaki, Comput. Phys. Comm. **181**, 1455 (2010).
[34] H. Shang, Z. Li, and J. Yang, J. Phys. Chem. A **114**, 1039 (2010).
[35] C. M. Goringe, E. Hernández, M. J. Gillan, and I. J. Bush, Comp. Phys. Commun. **102**, 1 (1997), 10.1016/S0010-4655(97)00029-5.
[36] D. J. Wales and M. P. Hodges, Chemical Physics Letters **286**, 65 (1998).
[37] O. F. Sankey and D. J. Niklewski, Phys. Rev. B **40**, 3979 (1989).
[38] J. Junquera, Ó. Paz, D. Sánchez-Portal, and E. Artacho, Physical Review B **64**, 235111 (2001).
[39] A. S. Torralba, M. Todorović, V. Brázdová, R. Choudhury, T. Miyazaki, M. J. Gillan, and D. R. Bowler, Journal of Physics: Condensed Matter **20**, 294206 (2008).
[40] A. Castro, A. Rubio, and M. Stott, Can. J. Phys. **81**, 1151 (2003).
[41] M. R. Jarvis, I. D. White, R. W. Godby, and M. C. Payne, Phys. Rev. B **56**, 14972 (1997).
[42] G. J. Martyna and M. E. Tuckerman, J. Chem. Phys. **110**, 2810 (1999).
[43] C. A. Rozzi, D. Varsano, A. Marini, E. K. U. Gross, and A. Rubio, Phys. Rev. B **73**, 205119 (2006).
[44] I. Dabo, B. Kozinsky, N. E. Singh-Miller, and N. Marzari, Phys. Rev. B **77**, 115139 (2008).
[45] H. Lee and M. E. Tuckerman, J. Chem. Phys. **129**, 224108 (2008).
[46] M. A. Watson and K. Hirao, **129**, 184107 (2008).
[47] K. Varga, Z. Zhang, and S. T. Pantelides, Phys. Rev. Lett. **93**, 176403 (2004).
[48] L. Genovese, T. Deutsch, A. Neelov, S. Goedecker, and G. Beylkin, J. Chem. Phys. **125**, 074105 (2006).
[49] L. Genovese, T. Deutsch, and S. Goedecker, J. Chem. Phys. **127**, 054704 (2007).
[50] G. Onida, L. Reining, R. W. Godby, R. Del Sole, and W. Andreoni, Phys. Rev. Lett. **75**, 818 (1995).
[51] P. E. Blochl, J. Chem. Phys. **103**, 7422 (1995).
[52] P. A. Schultz, Phys. Rev. B **60**, 1551 (1999).
[53] L. A. Truflandier and D. R. Bowler, unpublished results (2012).
[54] There is no restriction for the generation of the sampling points and the corresponding weights. It is well known that other nonlinear distributions allow to accelerate the convergence of numerical integration with respect to the size of the grid, mainly when we have to deal with singularities due to electronic cusps and nodal properties (for all–electron approaches) or Coulomb potentials. In this case, if one want to make an efficient use of FFT for the computation of Coulomb potential, we have to introduced transformation matrix to map the nonlinear distributions onto the FFT grid. We let this possibility open for future investigations.
[55] C. Skylaris, A. A. Mostofi, P. D. Haynes, C. J. Pickard, and M. C. Payne, Comput. Phys. Comm. **140**, 315 (2001).

[56] W. Kohn, Physical Review Letters **76**, 3168 (1996).

[57] E. Hernández, M. J. Gillan, and C. M. Goringe, Physical Review B **53**, 7147 (1996).